Electronic Journal of Biotechnology 39 (2019) 8–14

Contents lists available at ScienceDirect

Electronic Journal of Biotechnology

Research Article

Study of capability of nanostructured zero-valent iron and graphene oxide for bioremoval of trinitrophenol from wastewater in a bubble column bioreactor

Roya Bavandi [a], Mozhgan Emtyazjoo [a,*], Hasan Nasrollahzadeh Saravi [b], Fatemeh Yazdian [c], Mojgan Sheikhpour [d]

[a] Branch-Marine Science and Technology Faculty, Islamic Azad University North Tehran, Tehran, Iran
[b] Caspian Sea Ecology Research Center, Iranian Fisheries Sciences Research Institute, Agricultural Research, Education and Extension Organization, Tehran, Iran
[c] Department of Life Science Engineering, Faculty of New Sciences and Technologies, University of Tehran, Tehran, Iran
[d] Department of Mycobacteriology and Pulmonary Research, Microbiology Research Center, Pasteur Institute of Iran, Tehran, Iran

ARTICLE INFO

Article history:
Received 2 September 2018
Accepted 1 February 2019
Available online 19 February 2019

Keywords:
High bioremoval
Trinitrophenol
Oscillatoria cyanobacteria
Starch/nano zero-valent iron
Starch/GO/*Oscillatoria*
Phenolic compounds
Bioremediation
Cyanobacteria
Bioreactor
Bubble column

ABSTRACT

Background: Bioremoval of phenolic compounds using fungi and bacteria has been studied extensively; nevertheless, trinitrophenol bioremediation using modified *Oscillatoria* cyanobacteria has been barely studied in the literature.
Results: Among the effective parameters of bioremediation, algal concentration (3.18 $g \cdot L^{-1}$), trinitrophenol concentration (1301 $mg \cdot L^{-1}$), and reaction time (3.75 d) were screened by statistical analysis. *Oscillatoria* cyanobacteria were modified by starch/nZVI and starch/graphene oxide in a bubble column bioreactor, and their bioremoval efficiency was investigated. Modifiers, namely, starch/zero-valent iron and starch/GO, increased trinitrophenol bioremoval efficiency by more than 10% and 12%, respectively, as compared to the use of *Oscillatoria* cyanobacteria alone.
Conclusions: It was found that starch/nano zero-valent iron and starch/GO could be applied to improve the removal rate of phenolic compounds from the aqueous solution.
How to cite: Bavandi R, Emtyazjoo M, Saravi HN, et al. Study of nano-structure zero-valent iron and graphene-oxid capability onbioremoval of trinitrophenol from wastewater in a bubble column bioreactor. Electron J Biotechnol 2019;39. https://doi.org/10.1016/j.ejbt.2019.02.003.

1. Introduction

Water pollution has become a major problem in recent years [1]. In addition, trinitrophenol is a phenol derivative and is classified as the primary pollutant by US EPA (US Environmental Protection Agency). All phenolic compounds are widely used in industries such as pharmaceuticals and coal processing, production of polycarbonate resins, plastic, perfumes, textiles, and petroleum refineries [2,3]. Because of widespread production of these compounds and their health and environmental risks, many methods are applied for the detoxification of phenolic compounds that are pollutants in contaminated water; biological treatment for detoxification has turned out to be a promising and economical approach to deal with various recalcitrant pollutants such as trinitrophenol because of its merits such as low cost and environmental friendliness, but not versatile [4,5].

Bioremoval of phenolic compounds using fungi and bacteria has been studied extensively [6]; however, few efforts have been made to use algae for this purpose [2]. The biodegradation of phenol by microalgae occurs only under aerobic conditions. While some algae have a low tolerance to the acute toxicity of phenols, some others like cyanobacteria and eukaryotic microalgae (e.g., *Chlorella* sp., *Scenedesmus* sp., *Selenastrum capricornutum*, *Tetraselmis marina*, *Ochromonas danica*, *Lyngbya gracilis*, *Nostoc punctiforme*, *Oscillatoria animals*, and *Phormidium foveolamm*) are capable of biotransforming phenolic compounds. The phenol remediation ability of algae coupled with the potential applicability of the spent biomass as a biofuel feedstock and animal feed makes it a potential candidate for an environmentally sustainable process. *Anabaena cylindrica* degrades 2,4-dinitrophenol completely. *Chlorella* sp., *Scenedesmus obliquus*, and *Spirulina* sp. degraded phenol completely. *Chlorella vulgaris* and *Coenochloris pyrenoidosa* were found to degrade chlorophenol supplemented with zeolite up to 150 ppm [7].

Biotechnology often requires auxiliary processes, and addition of nanoparticles increases process efficiency; this is why electrons generated by nanoparticles may improve the enzymatic function and

* Corresponding author.
E-mail address: cyano.marine@gmail.com (M. Emtyazjoo).
Peer review under responsibility of Pontificia Universidad Católica de Valparaíso.

https://doi.org/10.1016/j.ejbt.2019.02.003

accelerate the electron transport chain [8]. Monometallic nanoparticles such as iron and gold nanoparticles, incorporation of two or more alloys, or use of different metals has greater effects on the bioproduction in addition to microorganisms. A study on the interaction of nanoparticles with microorganisms is of increasing interest. Different reports also have shown that nanoparticles can improve the growth of microorganisms and bioproduction [9,10]. Some microorganisms can employ Fe in different oxidation states as electron donors or acceptors in their energy metabolism [8,11]. Among all nanoparticles, nano-zero-valent iron (ZVI) particles are more popular for environmental remediation in both soil and groundwater treatment [12] because H_2 is produced during the corrosion of iron, which is considered to be a very suitable electron donor for microorganisms. In other words, zero-valent iron nanoparticles tend to condense rapidly that leads to loss of their reactivity. Hence, dispersion of Fe^0 nanoparticles is an essential step to improve the efficiency of their reaction [13]. Recently, the combination of biodegradation and iron-based nanoparticle for the reduction of nitrate [9,14] and phenol [7] has been investigated. By the way, numerous particle-stabilizing agents have been used, including carboxymethyl-cellulose, starch, and resin. Starch is a nontoxic, inexpensive, and substance biodegradable polysaccharide that can be used as an effective dispersant for iron nanoparticles. Certainly, it should be noted that results show difference in production and quality for different microorganisms, wherein each of them, when used alone, has shown different production results and quality of it. The application of nanostructures to remove biological pollutants with microorganisms has been commonly considered. The addition of iron-based nanoparticles accelerates the process of biological decomposition of pollutants, and during the oxidation of iron, electrons are produced, which can be used by microorganisms to regenerate pollutants [14,15,16].

Carbon nanotubes are another appropriate material for wastewater clarification [17]. Moreover, graphene oxide (GO), a two-dimensional carbon material, has attracted a great deal of attention [18]. Apart from the layered structure with a large theoretical specific surface area, GO nanosheets bear abundant oxygen-containing surface groups such as hydroxyl, epoxide, carbonyl, and carboxyl groups [19]. The presence of such groups not only allows the GO sheets to be well dispersed in water but also offers potential application as nanoscale substrates for electron transaction. For instance, GO has been employed as catalytic support applications [18,20].

Operating parameters are considered the main factor to improve the efficiency [21], and also reduce the time and cost of the process [2,7]. Therefore, it is necessary to design the process in terms of gathering information and experimental accuracy [2,22,23,24,25].

To accelerate bioproduction (such as biosurfactant production) and bioremoval (i.e., removal of nitrate and phenol-based components) through the use of nanotechnology and green engineering, application of metal nanoparticles with carbon-based nanostructures is a new study that has been welcomed and used by adding various types of metal nanoparticles to carbon-based nanostructures along with microorganisms, intended to produce bioproducts and remove pollutants [9,10,15]. This paper investigates the effect of starch/nano zero-valent iron and starch/GO separately as a modifier of *Oscillatoria* cyanobacteria on removal efficiency of trinitrophenol. For this goal, significant operating parameters have been screened and optimized, and the interaction of important factors has been studied.

2. Materials and methods

2.1. Cultivation and purification of Oscillatoria cyanobacteria

The cyanobacterium *Oscillatoria* is native to Iran and has been examined and cultivated by sampling the Persian Gulf. Information about the molecular identification of this fungus has been studied at the Pasteur Institute of Iran, whose results will be published shortly. First, to ensure that the sample was pure, purification of the cyanobacteria *Oscillatoria* by the plate agar method was carried out on a BG11 solid medium. The BG11 culture medium is the most common culture medium used for cyanobacteria and contains the following composition, in ($mg \cdot L^{-1}$): 75 $MgSO_4$, 150 $NaNO_3$, 6 $C_6H_8O_7$, 36 $CaCl_2 \cdot 2H_2O$, 1 EDTA, 6 Ferric ammonium citrate, 1 Trace metal mix solution, and 20 $NaCO_3$ [26].

To prepare the BG-11 medium, 30 g of agar was dissolved in 1 L of BG-11 liquid medium and autoclaved. Thus, the autoclaved medium was transferred to Petri dishes. After cooling the solid medium, the cyanobacterial colonies were cultured on a loop using sewing. This work was repeated several times for obtaining pure colonies of cyanobacteria, and each time, colonies that had to be re-cultured were selected by slalom and microscopic examination. To increase the desired cyanobacteria and obtain sufficient amount of it for carrying out the test steps, after ensuring that the colonies in solid culture are pure, the colonies are transferred to the BG11 liquid medium, grown in an aeration chamber and continuous light radiation, and maintained at a temperature of 28 ± 2°C.

2.1.1. Bubble column preparation and experimentation

The bioreactor is a device in which chemical and biological processes are monitored carefully, and the operating and environmental parameters are well controlled [27].

The bioremediation of trinitrophenol using *Oscillatoria* was upscaled in a bubble column photobioreactor of capacity 300 mL with a 200 mL working volume because it creates less shear stress; hence, it is useful for the growth of organized structures. The bubble column bioreactor used in this study was made of a glass column (Corning glass, height 35 cm and diameter 10 cm) of 500 mL capacity. In the upper part of the bioreactor, two ducts were designed for air outlet and sampling port, and the air inlet flow rate in the reactor was set at the bottom of the bubble column bioreactor where bubbles were interred through a sparger [28]. The bioreactor operated under a fluorescent lamp at wavelengths 400–700 nm (8 watts, center of the bioreactor) at a temperature of 30 ± 1°C. The trinitrophenol removal process at different concentrations ($mg \cdot L^{-1}$) (300, 650, 1000, 1350, and 1600) using different amounts of the oscillator ($g \cdot L^{-1}$) (1, 2, 3, 4, and 5) and in the predicted time intervals (days) (1, 2, 3, 4, and 5) was investigated in the bioreactor, and at the end of each experiment, the concentration of trinitrophenol in the aqueous was determined by the colorimetric method using a spectrophotometer at 365 nm. Loop bioreactors are characterized by a directed circulation flow, which can be driven in fluid or fluidized systems by a propeller or jet drive and most typically in gas–liquid systems using a bubble drive or liquid pump. They are particularly suitable for fluid systems requiring high-dispersion priority.

On the other hand, their simple constructions and operation result in low investment and operational costs. The use of multistage bubble

Table 1
Plackett–Burman design matrix for five variables with actual values along with experimentally obtained trinitrophenol biodegradation.

Oscillatoria concentration ($mg \cdot L^{-1}$)	Trinitrophenol concentration ($mg \cdot L^{-1}$)	Nitrogen source	Source of phosphorus	Reaction time	Trinitrophenol degradation (%)
1	−1	1	−1	−1	88.4
1	1	−1	1	−1	81.4
−1	1	1	−1	1	70.1
1	−1	1	1	−1	85.0
1	1	−1	1	1	88.5
1	1	1	−1	1	85.3
−1	1	1	1	−1	66.0
−1	−1	1	1	1	85.1
−1	−1	−1	1	1	83.2
1	−1	−1	−1	1	88.5
−1	1	−1	−1	−1	66.6
−1	−1	−1	−1	−1	80.0

Table 2
Central composite design for three independent variables and their predicted and observed results.

Run	Algal concentration	Trinitrophenol concentration	Reaction time	Trinitrophenol biodegradation (%)	
				Observed	Predicted
1	−1.00	−1.00	−1.00	54	55.96
2	1.00	−1.00	−1.00	65	72.88
3	−1.00	1.00	−1.00	43	40.0
4	1.00	1.00	−1.00	46	56.92
5	−1.00	−1.00	1.00	61	66.00
6	1.00	−1.00	1.00	89	82.92
7	−1.00	1.00	1.00	69	68.04
8	1.00	1.00	1.00	87	84.96
9	−1.68	0.00	0.00	48	47.94
10	1.68	0.00	0.00	81	76.36
11	0.00	−1.68	0.00	88	84.48
12	0.00	1.68	0.00	74	72.79
13	0.00	0.00	−1.68	54	45.14
14	0.00	0.00	1.68	73	77.13
15	0.00	0.00	0.00	89	88.80

reactors may reduce the cost of mixing and overcome poor reaction kinetics and to achieve continuous growth and regeneration of the biocatalyst in the same system rather than in a separate reactor. In the design of the draft tube reactor, high oxygen utilization is an advantage over mechanically stirred bioreactors. Therefore, if whole cells are used as biocatalyst, then less shear damage would occur [28,29].

2.2. Experimental design and data analysis

2.2.1. Screening of significant factors and optimal level

The Plackett–Burman Design (PBD) is an effective screening method to identify important factors [30]. Three influencing factors, namely, algal concentration ($g \cdot L^{-1}$) (X_1), trinitrophenol concentration ($g \cdot L^{-1}$) (X_2), and reaction time (days) (X_3), have been specified, and each of these independent variables is evaluated at five levels ($-\alpha$, -1, 0, $+1$, and $+\alpha$). A total of 12 runs were carried out. The full factorial CCD has been used to the optimal level of significant factors.

2.2.2. Statistical analysis

The analysis of variance (ANOVA) was used for statistical analysis. To measure the fit of the regression model, Fisher test (F-test), its associated probability P (F), and the coefficient of determination (R^2) were used. Further, to evaluate the interaction between the influencing parameters, response surface and contour plots of predicted responses of the model were used.

2.3. Synthesis of starch/nano zero-valent iron and starch/graphene oxide

In this study, the common liquid-phase method was used to reduce the ferric ions with potassium borohydride to synthesize nano-zero-valent iron [31]. To produce ferric ion solution, ferric chloride heptahydrate (6 g) was dissolved in water, with ethanol as the dispersing agent in a ratio of 1:3, and stirred at 250 rpm. Water-soluble starch (2 g) was then added to the solution and stirred for 30 min. This was followed by adding a freshly prepared KBH_4 solution (5.4 g of KBH_4 in 30 mL of ethanol and 20 mL of water solution) to the medium and stirring for another 60 min. To prevent the oxidation of S-nZVI, the process described was performed under inert atmosphere of N_2 gas [17]. In the end, the produced suspension was filtered, and the black nanoscale obtained was washed three times using distilled water, ethanol, and acetone [32].

GO was synthesized from graphite powder by a modified Hummer's method. In brief, 1 g of graphite and 0.5 g of sodium nitrate were mixed followed by the addition of 23 mL of concentrated sulfuric acid under constant stirring. After 1 h, 3 g of potassium permanganate ($KMnO_4$) was added gradually to the above solution while keeping the temperature less than 20°C to prevent overheating and explosion. The mixture was stirred at 35°C for 12 h, and the resulting solution was diluted by adding 500 mL of water under vigorous stirring. To ensure the completion of the reaction with $KMnO_4$, the suspension was further treated with 30% H_2O_2 solution (5 mL). The resulting mixture was washed with HCl and H_2O successively, followed by filtration and drying; GO sheets were thus obtained [18]. Size of starch/nZVI and starch/GO were analyzed by TEM and SEM.

3. Results and discussion

3.1. Screening of significant factors by statistical design

Five variables affecting the biodegradation of trinitrophenol by *Oscillatoria* have been studied using the Plackett–Burman Design. The results of the 12-design experiment and the corresponding response are shown in Table 1.

According to the magnitude of the coefficient for significance ($P < 0.05$), it turns out that among the five variables studied, *Oscillatoria* concentration, trinitrophenol concentration, and reaction time have been known as a significant factor. These three parameters have also been reported in a similar study, which was performed to biodegrade phenol from aqueous solution using microalga *Chlorella pyrenoidosa* [2].

3.2. Optimization of significant factors by RSM

The central composite design has been used to optimize the significant parameters from PBD. Each variable has been examined at five levels, and results are shown in Table 2.

Trinitrophenol biodegradation efficiency was described with a second-order polynomial equation, by applying multiple regression analysis on the experimental data:

$$Y = 88.80 + 8.46A - 3.48B + 9.52C + 4.00A.C + 4.50B.C - 9.44A^2 - 3.6B^2 - 9.80C^2 \quad \text{[Equation 1]}$$

where, Y is the predicted trinitrophenol biodegradation (%) and A, B, and C are the values of initial algal concentration, initial trinitrophenol concentration, and reaction time, respectively.

Consequently, the optimum situation for maximum removal of trinitrophenol by *Oscillatoria* cyanobacteria was found to be 3.18 $g \cdot L^{-1}$ algal concentration, 1301 $mg \cdot L^{-1}$ initial trinitrophenol concentration,

Table 3
Summary of investigations on the biodegradation of phenol and its derivatives.

Contaminant	Microorganism	Operational parameters	Efficiency	Ref.
Phenol	*Acinetobacter calcoaceticus*	Initial 800 $mg \cdot L^{-1}$ phenol within 48 h	91.6%	[33]
Phenol	*Chlorella pyrenoidosa*	The algal concentration of 4 $g \cdot L^{-1}$, phenol concentration of 0.8 $g \cdot L^{-1}$, and reaction time of 4 d.	97%	[2]
Phenol	*Bacillus pumilus*	pH 7.07, temperature 29.3°C, phenol 227.4 $mg \cdot L^{-1}$, inoculum size 6.3% (v/v), $(NH_4)_2SO_4$ 392.1 $mg \cdot L^{-1}$.	99.99%	[7]
Phenol	*Microbial consortium*	Initial concentration 1000 $mg \cdot L^{-1}$, temperature 35°C, pH 7, and incubation time of 96 h	99%	[24]
Phenol and p-nitrophenol	*Bacillus cereus*	Temperature 37°C and aerobic condition, *vgb* gene	100%	[34]
p-Nitrophenol	*Pseudomonas aeruginosa*	maximum concentration of 500 $mg \cdot L^{-1}$ within 24 h in a mineral salt medium		[35]
2,6-Dibromo-4 nitrophenol	*Cupriavidus* sp. strain CNP8	concentrations of up to 0.7 Mm		[36]

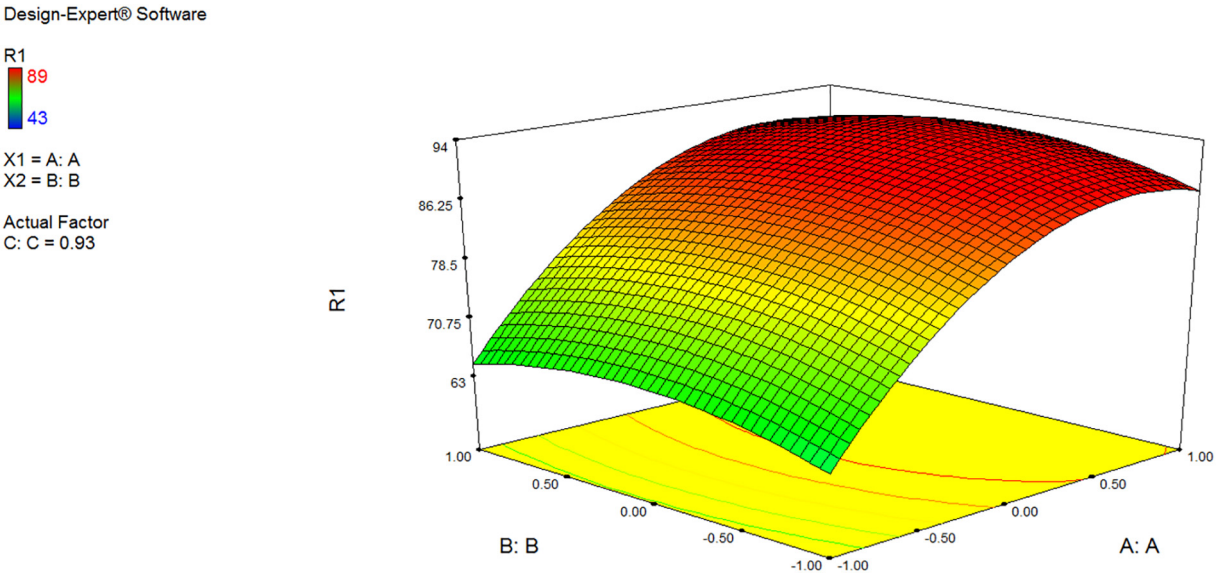

Fig. 1. Three-dimensional response surface plots of the effect of variable interactions on trinitrophenol bioremediation by the cyanobacteria *Oscillatoria*: initial algal concentration (A) and initial trinitrophenol (B).

and 3.75 d of reaction time. Under optimal predicted conditions, the percentage of trinitrophenol removal was 88.89%. In a similar study that was carried out to remove phenol using *Bacillus fusiformis*, the percentage of pollutant removal was expected to be 60% [37]. Priyadharshini and Bakthavatsalam [2] reported removal of 97% of phenol from water using *C. pyrenoidosa*, with an algal concentration of 4 $g \cdot L^{-1}$, phenol concentration of 0.8 $g \cdot L^{-1}$, and reaction time of 4 d. Patil and Jena [7] reported 99.98% biodegradation of phenol by *Bacillus pumilus* isolated from crude oil spillage under optimized conditions. The report states that there is no significant change in the percentage of phenol degradation by changing the concentration of phenol in comparison with other parameters (Table 3) [7].

The adequacy of the model has been assessed using analysis of variance (ANOVA). The "F-value" of the model was 26.51 and the *P*-value <0.0001, suggesting that the model was highly significant. According to Equation 1] and *P*-value, algal concentration (A) and reaction time (C) have a significant ($P < 0.05$) positive relationship with trinitrophenol biodegradation, while the second-order main effect of algal concentration (A^2) and reaction time (C^2) has a significant ($P < 0.05$) negative relationship with trinitrophenol biodegradation.

Regression model has a correlation coefficient value (R^2) of 0.9507, which shows that experimental results are well suited to the quadratic model.

3.3. Mutual interactions between the significant factors

To study the process parameters, RSM was used. The diagrams were plotted according to Equation 1] so that one of the parameters remained constant under optimal conditions, and the interaction of two other parameters on the removal efficiency was studied. In all diagrams, a peak point is observed, which indicates the existence of optimal conditions.

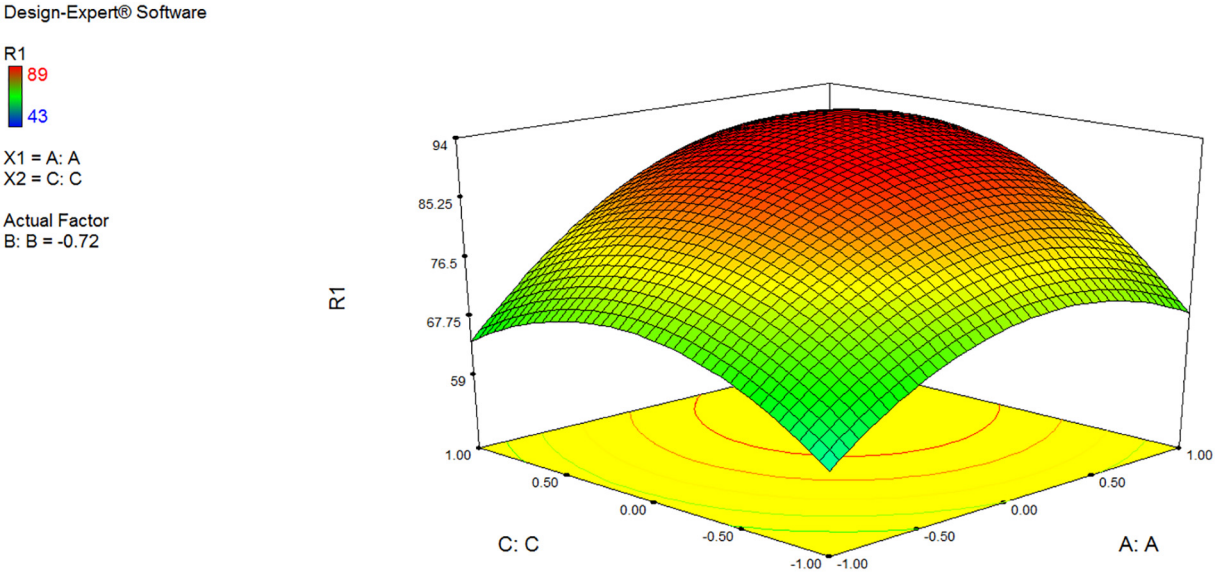

Fig. 2. Three-dimensional response surface plots of the effect of variable interactions on trinitrophenol bioremediation by the cyanobacteria *Oscillatoria*: initial algae concentration (A) and reaction time (C).

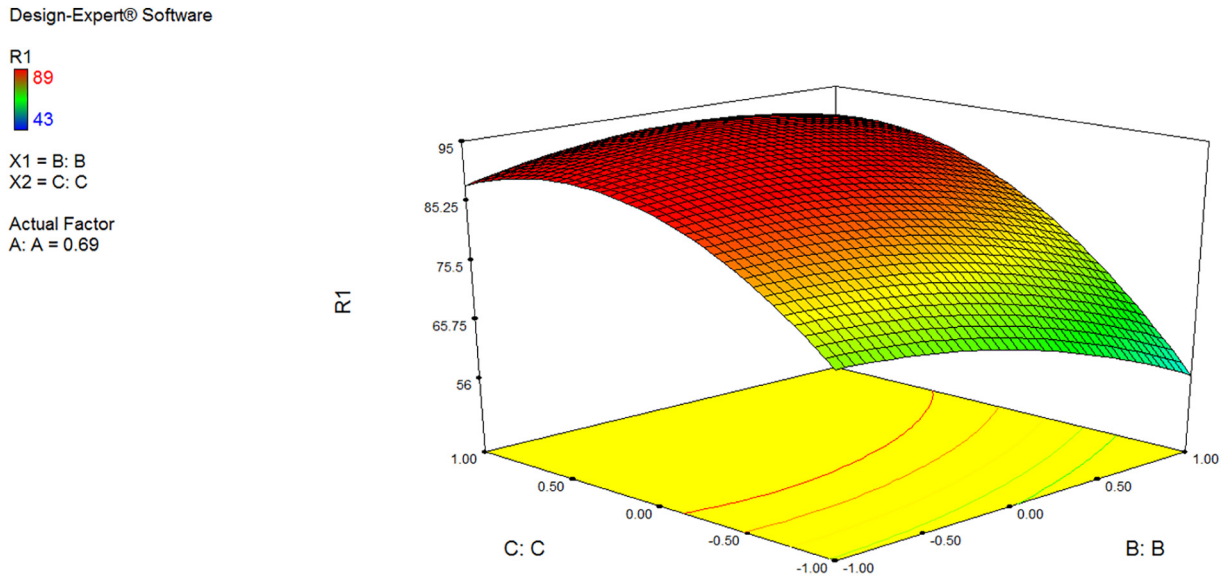

Fig. 3. Three-dimensional response surface plots of the effect of variable interactions on Trinitrophenol bioremediation by *Oscillatoria* cyanobacteria: initial trinitrophenol concentration (B) and reaction time (C).

The effects of *Oscillatoria* concentration (A) and trinitrophenol concentration (B) on phenol remediation while keeping reaction time (C) constant at optimum level are shown in Fig. 1. Removal efficiency was found to be increased by increasing the number of algae at constant initial concentrations of trinitrophenol. However, for constant *Oscillatoria* concentration, increase in initial concentrations of pollutants does not indicate a significant role in the removal percentage. This behavior is probably because, in the predicted time interval, the trinitrophenol was degraded by algae and converted to intermediate materials.

The interactions of reaction time (C) and *Oscillatoria* concentration (A) on pollutant removal percentage in the constant and optimal initial trinitrophenol concentration (B) are shown in Fig. 2. At constant time intervals, by increasing the number of algae, the percentage of pollutant removal initially increased and continued to decrease. On the other hand, for a fixed *Oscillatoria* concentration, increase in time initially increases the percentage of pollutant removal and further reduces this amount.

In Fig. 3 the interaction effect of the two parameters of the trinitrophenol concentration (B) and the reaction time (C) in the pollutants' removal percentage while the algae concentration (A) under optimal conditions has been studied. At constant time intervals, an increase in the initial concentration of trinitrophenol in the percentage of pollutant removal is ignorable. While for constant concentrations of contaminants, by increasing the time, removal efficiency is increased. This behavior is due to the fact that in the constant initial concentrations of trinitrophenol, with increasing exposure time, more active sites of *Oscillatoria* are involved in the process, and more pollutants can be exposed to biological processes. When the exposure period remains constant, by increasing initial concentrations of trinitrophenol, there is not enough time to encounter all pollutant particles to active algae sites, and as a result, the percentage of pollutant removal remains almost constant or reduces. Resemblance behavior is reported in other studies that have been carried out to investigate the modeling and optimization of phenol degradation over copper-doped titanium dioxide photocatalyst [38].

3.4. Characterization of starch/Fe^0

Transmission electron microscopy images were used to determine the morphology, size, and distribution of nanoparticles [11]. As shown in Fig. 4, nZVI has a light gray shell around the spherical black core, which is the reason why the material is covered with starch. Moreover, the nanoparticles have a spherical shape and size ranging from 5 to 35 nm [32].

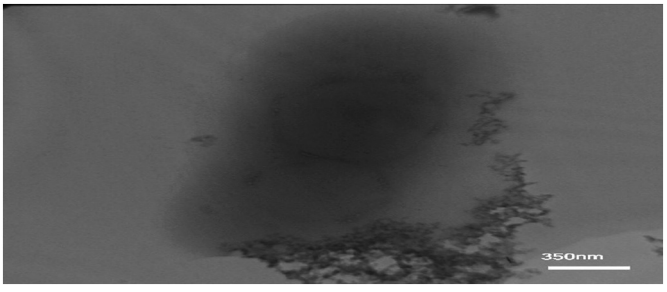

Fig. 4. Transmission electron microscopy (TEM) images of S-nZVI [32].

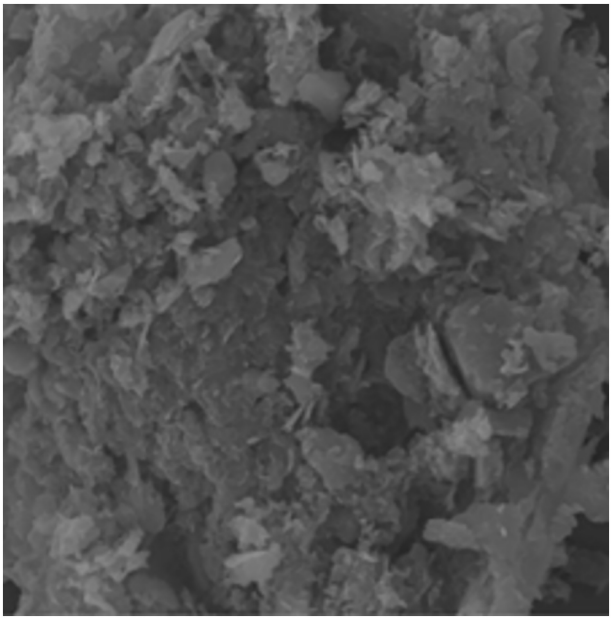

Fig. 5. SEM micrograph of GO.

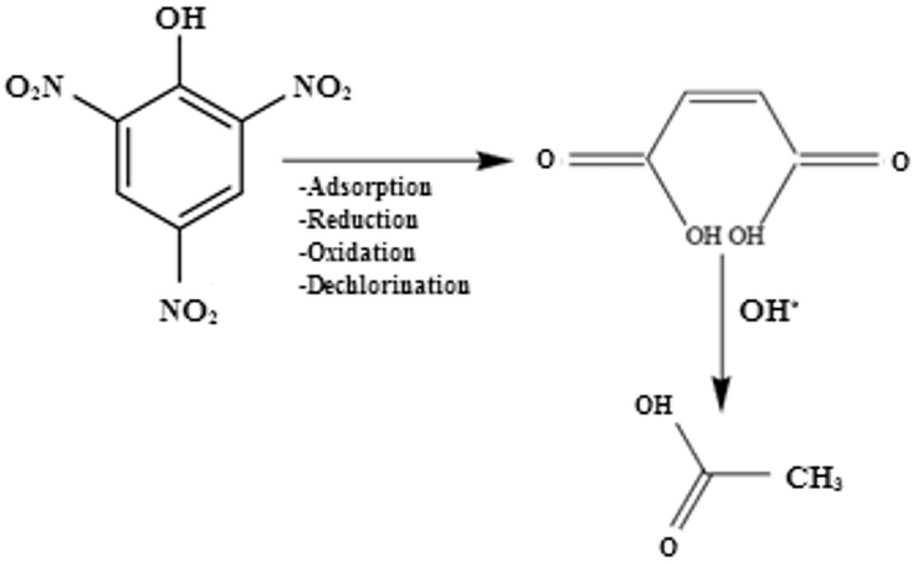

Fig. 6. Schematic of biodegradation of phenol-based compounds by the cyanobacteria *Oscillatoria*.

3.5. Characterization of starch/graphene oxide

The results were obtained from the preliminary analysis of GO and are shown in Fig. 5. As shown, the synthesized GO was mostly single layered with a topographic height of 2 nm.

3.6. Starch/nano-zero-valent iron and starch/GO as enhancers for trinitrophenol bioremoval

Under optimal conditions, 1 $g \cdot L^{-1}$ of nanoscale zero-valent iron was added to the culture, and under the same conditions, the percentage of removal of trinitrophenol was studied. The observations showed that by adding nanoscale zero-valent iron to the environment compared to the environment when it is not used, the removal efficiency was improved from 88.89% to 97.61%. Phenol-based components degraded by the cyanobacteria *Oscillatoria* are shown in Fig. 6. The contact between the organic contaminant and reactive site on the iron nanoparticle surface directly determines TNP removal by the nanoparticle. TNP was adsorbed on the reactive iron particle surface after being spread through the solution. Then, iron nanoparticles as electron donors were corroded following the occurrence of effective contact between them and molecular TCP. Further, hydrogen peroxide could be created by iron corrosion in the presence of oxygen. As a result, strong oxidants like OH• species could be produced by the reaction between Fe^2 and hydrogen peroxide. The TNCP bond was broken by the organic pollutant degradation with the help of the hydroxyl radical as soon as the TNP was adsorbed onto the nanoparticle surface [31]. The ferrous ions from iron-oxide corrosion were able to promote the synthesis of key enzymes [11].

Additionally, when using starch/GO as an enhancer, the bioremoval efficiency of the pollutant reached 100%. Some studies investigated the influence of iron-based nanoparticles such as nanoscale zero-valent iron (nZVI) in biodegradation. Vilardi et al. [8] believed that the produced H_2 in corrosion of iron acts as an electron donor, and in addition, it is a substantial energy source for microorganisms [11,17, 39]. Further, a similar study claimed that the use of iron-based nanoparticles adhered to the surface of *B. fusiformis* (BFN) [40]. Kim et al. [41] studied the degradation of polybrominated diphenyl ethers by sequential treatment with nanoscale zero-valent iron and aerobic biodegradation. Li et al. [42] reported that nanoscale zero-valent iron supported on organobentonite had enhanced performance on removing chlorophenols. They claimed that maximum removal efficiencies of 2-chlorophenols, 2,4-dichlorophenol, 2,4,6-trichlorophenol, and pentachlorophenol by nZVI/CTMA-Bent were 88.2%, 91.1%, 92.6%, and 94.1%, respectively [42]. In a similar report, it has been attempted to enhance the removal of pentachlorophenol by a nanoscale zero-valent iron immobilized on organobentonite. Li et al. [43] reported that the percentage removal of pentachlorophenol by nZVI/CTMA-Bent reached 96.2% after 120 min. Cheng et al. [44] investigated the effect of the zero-valent iron/H_2O_2 system on pentachlorophenol removal from water. The report states that after 1 h, the pentachlorophenol degradation process was completed using the zero-valent iron/H_2O_2 system. In another study, removal of 4-chlorophenol by granular activated carbon/nanoscale zero-valent iron has been studied. It is claimed that maximum efficiency for pollutant removal was 97.23% [31].

4. Conclusion

The first objective of this study was to identify the effective factors on trinitrophenol bioremediation using the cyanobacteria *Oscillatoria* with starch/nano zero-violet iron and starch/GO to achieve the highest removal rate. Initial trinitrophenol concentration, algal concentration, and reaction time were identified as effective factors, and their mutual interaction was investigated. Nevertheless, removal efficiency was approximately 88.89% under optimal conditions. In the following, starch/nano zero-valent iron and starch/GO were used to improve the removal rate of pollutants from the solution; therefore, removal efficiency increased by 9.81% and 12.49% respectively.

Conflict of interest

The authors declare that they have no conflict of interest.

References

[1] Vuppala S, Di Palma L, Cianfrini C, et al. Flocculation and nanofiltration processes with insight of fouling phenomena for the treatment of olive mill wastewater. Chem Eng Trans 2017;60:265–70.
[2] Priyadharshini SD, Bakthavatsalam AK. Optimization of phenol degradation by the microalga *Chlorella pyrenoidosa* using Plackett–Burman Design and Response Surface Methodology. Bioresour Technol 2016;207:150–6. https://doi.org/10.1016/j.biortech.2016.01.138 PMid:26878360.
[3] Kiliç NK, Dönmez G. Dual bioremediation of phenol and Cr (VI) by mixed microbial cultures in the presence of molasses. Water Sci Technol 2017;75:2883–90. https://doi.org/10.2166/wst.2017.163 PMid:28659528.

[4] Liang J, Li W, Zhang H, et al. Coaggregation mechanism of pyridine-degrading strains for the acceleration of the aerobic granulation process. Chem Eng J 2018;338: 176–83. https://doi.org/10.1016/j.cej.2018.01.029.
[5] Wang J, Jiang X, Liu X, et al. Microbial degradation mechanism of pyridine by *Paracoccus* sp. NJUST30 newly isolated from aerobic granules. Chem Eng J 2018; 344:86–94. https://doi.org/10.1016/j.cej.2018.03.059.
[6] Pradeep NV, Anupama S, Navya K, et al. Biological removal of phenol from wastewaters: A mini review. Appl Water Sci 2015;5:105–12. https://doi.org/10.1007/s13201-014-0176-8.
[7] Patil SS, Jena HM. Statistical optimization of phenol degradation by *Bacillus pumilus* OS1 using Plackett–Burman design and response surface methodology. Arab J Sci Eng 2015;40:2141–51. https://doi.org/10.1007/s13369-015-1765-z.
[8] Vilardi G, Sebastiani D, Miliziano S, et al. Heterogeneous nZVI-induced Fenton oxidation process to enhance biodegradability of excavation by-products. Chem Eng J 2018;335: 309–20. https://doi.org/10.1016/j.cej.2017.10.152.
[9] Rajab Beigy M, Rasekh B, Yazdian F, et al. High nitrate removal by starch-stabilized Fe^0 nanoparticles in aqueous solution in a controlled system. Eng Life Sci 2017: 1–30. https://doi.org/10.1002/elsc.201700127.
[10] Sahebnazar Z, Mowla D, Karimi G, et al. Zero-valent iron nanoparticles assisted purification of rhamnolipid for oil recovery improvement from oily sludge. J Environ Chem Eng 2018;6:917–22. https://doi.org/10.1016/j.jece.2017.11.043.
[11] Jiang X, Chen Y, Hou C, et al. Promotion of para-chlorophenol reduction and extracellular electron transfer in an anaerobic system at the presence of iron-oxides. Front Microbiol 2018;9. https://doi.org/10.3389/fmicb.2018.02052.
[12] Di Palma L, Verdone N, Vilardi G. Kinetic modeling of Cr (VI) reduction by nZVI in soil: The influence of organic matter and manganese oxide. Bull Environ Contam Toxicol 2018:1–6. https://doi.org/10.1007/s00128-018-2394-5.
[13] Mofradnia SR, Tavakoli Z, Yazdian F. Fe/starch nanoparticle - *Pseudomonas aeruginosa*: Bio-physiochemical and MD studies. Int J Biol Macromol 2018;117: 51–61. https://doi.org/10.1016/j.ijbiomac.2018.04.191.
[14] Mofradnia SRSR, Ashouri R, Tavakoli Z, et al. Effect of zero-valent iron/starch nanoparticle on nitrate removal using MD simulation. Int J Biol Macromol 2018; 121:727–33. https://doi.org/10.1016/j.ijbiomac.2018.09.183.
[15] Alamdar N, Rasekh B, Yazdian F. Effects of Fe/SDS and Au nanoparticles on *Pseudomonas aeroginosa* bacterial growth and biosurfactant production. IET Nanobiotechnol 2018: 26–8. https://doi.org/10.1049/iet-nbt.2016.0260.
[16] Etemadi N, Sepahy AA, Mohebali G, et al. Enhancement of bio-desulfurization capability of a newly isolated thermophilic bacterium using starch/iron nanoparticles in a controlled system. Int J Biol Macromol 2018;120:1801–9. https://doi.org/10.1016/j.ijbiomac.2018.09.110.
[17] Khezri A, Karimi A, Yazdian F, et al. Molecular dynamic of curcumin/chitosan interaction using a computational molecular approach: Emphasis on biofilm reduction. Int J Biol Macromol 2018;114:972–8. https://doi.org/10.1016/j.ijbiomac.2018.03.100.
[18] Vilardi G, Mpouras T, Dermatas D, et al. Nanomaterials application for heavy metals recovery from polluted water: The combination of nano zero-valent iron and carbon nanotubes. Competitive adsorption non-linear modeling. Chemosphere 2018;201: 716–29. https://doi.org/10.1016/j.chemosphere.2018.03.032. PMid:29547860.
[19] Mohammadnejad J, Yazdian F, Omidi M, et al. Graphene oxide/silver nanohybrid: Optimization, antibacterial activity and its impregnation on bacterial cellulose as a potential wound dressing based on GO–Ag nanocomposite-coated BC. Eng Life Sci 2018;18:298–307. https://doi.org/10.1002/elsc.201700138.
[20] Ashouri R, Ghasemipoor P, Rasekh B, et al. The effect of ZnO-based carbonaceous materials for degradation of benzoic pollutants: A review. Int J Environ Sci Technol 2018:1–12. https://doi.org/10.1007/s13762-018-2056-5.
[21] Hur J, Shin J, Yoo J, et al. Competitive adsorption of metals onto magnetic graphene oxide: comparison with other carbonaceous adsorbents. Sci World J 2015;836287. https://doi.org/10.1155/2015/836287.
[22] Puértolas B, Mayoral Á, Arenal R, et al. High-temperature stable gold nanoparticle catalysts for application under severe conditions: The role of TiO2 nanodomains in structure and activity. ACS Catal 2015;5:1078–86. https://doi.org/10.1021/cs501741u.
[23] Vilardi G, Di Palma L, Verdone N. On the critical use of zero valent iron nanoparticles and Fenton processes for the treatment of tannery wastewater. J Water Process Eng 2018;22:109–22. https://doi.org/10.1016/j.jwpe.2018.01.011.
[24] Sivasubramanian S, Namasivayam SKR. Phenol degradation studies using microbial consortium isolated from environmental sources. J Environ Chem Eng 2015;3: 243–52. https://doi.org/10.1016/j.jece.2014.12.014.
[25] Wong KK, Quilty B, Hamzah A, et al. Phenol biodegradation and metal removal by a mixed bacterial consortium. Biorem J 2015;19:104–12. https://doi.org/10.1080/10889868.2014.995368.
[26] Jabeen H, Iqbal S, Anwar S, et al. Optimization of profenofos degradation by a novel bacterial consortium PBAC using response surface methodology. Int Biodeter Biodegr 2015;100:89–97. https://doi.org/10.1016/j.ibiod.2015.02.022.
[27] Silveira JE, Zazo JA, Pliego G, et al. Electrochemical oxidation of landfill leachate in a flow reactor: Optimization using response surface methodology. Environ Sci Pollut Res 2015; 22:5831–41. https://doi.org/10.1007/s11356-014-3738-2 PMid:25339535.
[28] Allen MM, Stanier RY. Growth and division of some unicellular blue-green algae. Microbiology 1968;51:199–202.
[29] Patra N, Srivastava AK. Mass production of artemisinin using hairy root cultivation of *Artemisia annua* in bioreactor. Bioprocess Plant Vitr Syst 2017:1–17. https://doi.org/10.1007/978-3-319-32004-5_20-1.
[30] Khazeni S, Hatamian-Zarmi A, Yazdian F, et al. Production of nanocellulose in miniature-bioreactor: Optimization and characterization. Prep Biochem Biotechnol 2017;47:371–8. https://doi.org/10.1080/10826068.2016.1252923 PMid:27824292.
[31] Karimi E, Jeffryes C, Yazdian F, et al. DBT desulfurization by decorating *Rhodococcus erythropolis* IGTS8 using magnetic Fe3O4 nanoparticles in a bioreactor. Eng Life Sci 2017;17:528–35. https://doi.org/10.1002/elsc.201600080.
[32] Ungureanu CP, Favier L, Bahrim G, et al. Response surface optimization of experimental conditions for carbamazepine biodegradation by *Streptomyces* MIUG 4.89. N Biotechnol 2015;32:347–57. https://doi.org/10.1016/j.nbt.2014.12.005 PMid:25556120.
[33] Liu S, Tian J, Wang L, et al. One-pot synthesis of CuO nanoflower-decorated reduced graphene oxide and its application to photocatalytic degradation of dyes. Cat Sci Technol 2012;2:339–44. https://doi.org/10.1039/C1CY00374G.
[34] Vélez-Lee AE, Cordova-Lozano F, Bandala ER, et al. Cloning and expression of vgb gene in *Bacillus cereus*, improve phenol and p-nitrophenol biodegradation. Phys Chem Earth, Parts A/B/C 2016;91:38–45. https://doi.org/10.1016/j.pce.2015.10.017.
[35] Zheng Y, Liu Deli, Liu Shiwang, et al. Kinetics and mechanisms of p-nitrophenol biodegradation by *Pseudomonas aeruginosa* HS-D38. J Environ Sci 2009;21:1194–9. https://doi.org/10.1016/S1001-0742(08)62403-1.
[36] Fu M, Li Y, Wu S, et al. Sol–gel preparation and enhanced photocatalytic performance of Cu-doped ZnO nanoparticles. Appl Surf Sci 2011;258:1587–91. https://doi.org/10.1016/j.apsusc.2011.10.003.
[37] Majlesi M, Hashempour Y. Removal of 4-chlorophenol from aqueous solution by granular activated carbon/nanoscale zero valent iron based on Response Surface Modeling. Arch Environ Prot 2016;43:13–25. https://doi.org/10.1515/aep-2017-0035.
[38] Sohrabi S, Akhlaghian F. Modeling and optimization of phenol degradation over copper-doped titanium dioxide photocatalyst using response surface methodology. Process Saf Environ Prot 2016;99:120–8. https://doi.org/10.1016/j.psep.2015.10.016.
[39] Vilardi G, Ochando-Pulido JM, Verdone N, et al. On the removal of hexavalent chromium by olive stones coated by iron-based nanoparticles: Equilibrium study and chromium recovery. J Clean Prod 2018;190:200–10. https://doi.org/10.1016/j.jclepro.2018.04.151.
[40] Kuang Y, Zhou Y, Chen Z, et al. Impact of Fe and Ni/Fe nanoparticles on biodegradation of phenol by the strain *Bacillus fusiformis* (BFN) at various pH values. Bioresour Technol 2013;136:588–94. https://doi.org/10.1016/j.biortech.2013.03.018 PMid:23567735.
[41] Kim Y, Murugesan K, Chang Y, et al. Degradation of polybrominated diphenyl ethers by a sequential treatment with nanoscale zero valent iron and aerobic biodegradation. J Chem Technol Biotechnol 2012;87:216–24. https://doi.org/10.1002/jctb.2699.
[42] Li Y, Zhang Y, Li J, et al. Enhanced reduction of chlorophenols by nanoscale zerovalent iron supported on organobentonite. Chemosphere 2013;92:368–74. https://doi.org/10.1016/j.chemosphere.2013.01.030 PMid:23399303.
[43] Li Y, Zhang Y, Li J, et al. Enhanced removal of pentachlorophenol by a novel composite: Nanoscale zero valent iron immobilized on organobentonite. Environ Pollut 2011;159: 3744–9. https://doi.org/10.1016/j.envpol.2011.07.016 PMid:21906860.
[44] Cheng R, Cheng C, Liu G, et al. Removing pentachlorophenol from water using a nanoscale zero-valent iron/H2O2 system. Chemosphere 2015;141:138–43. https://doi.org/10.1016/j.chemosphere.2015.06.087 PMid:26184790.